Evaluation of Battery Management Systems for Electric Vehicles Using Traditional and Modern Estimation Methods.

Noreen, Muhammad Talha Mumtaz, Fouladfar, Mohammad Hossein and Saeed, Nagham ORCID logoORCID: https://orcid.org/0000-0002-5124-7973 (2024) Evaluation of Battery Management Systems for Electric Vehicles Using Traditional and Modern Estimation Methods. Network, 4 (4). pp. 586-608.

http://dx.doi.org/10.3390/network4040029

network

MDPI

Article

Evaluation of Battery Management Systems for Electric Vehicles Using Traditional and Modern Estimation Methods

Muhammad Talha Mumtaz Noreen [1,*], Mohammad Hossein Fouladfar [2] and Nagham Saeed [1]

[1] Department of Computing and Engineering, University of West London, London W5 5RF, UK; nagham.saeed@uwl.ac.uk

[2] Department of Engineering and Applied Sciences, University of Bergamo, 24044 Dalmine, Italy; mohammad.fouladfar@unibg.it

* Correspondence: talhamumtaz501@gmail.com; Tel.: +44-7438421375

Abstract: This paper presents the development of an advanced battery management system (BMS) for electric vehicles (EVs), designed to enhance battery performance, safety, and longevity. Central to the BMS is its precise monitoring of critical parameters, including voltage, current, and temperature, enabled by dedicated sensors. These sensors facilitate accurate calculations of the state of charge (SOC) and state of health (SOH), with real-time data displayed through an IoT cloud interface. The proposed BMS employs data-driven approaches, like advanced Kalman filters (KF), for battery state estimation, allowing continuous updates to the battery state with improved accuracy and adaptability during each charging cycle. Simulation tests conducted in MATLAB's Simulink across multiple charging and discharging cycles demonstrate the superior accuracy of the advanced Kalman filter (KF), in handling non-linear battery behaviours. Results indicate that the proposed BMS achieves a significantly lower error margin in SOC tracking, ranging from 0.32% to 1%, compared to traditional methods with error margins up to 5%. These findings underscore the importance of integrating robust sensor systems in BMSs to optimise EV battery management, reduce maintenance costs, and improve battery sustainability.

Keywords: battery management system; state of charge estimation; state of health estimation; coulomb counting; extended Kalman filter; unscented Kalman filter; internet of things; electric vehicle

Citation: Mumtaz Noreen, M.T.; Fouladfar, M.H.; Saeed, N. Evaluation of Battery Management Systems for Electric Vehicles Using Traditional and Modern Estimation Methods. *Network* **2024**, *4*, 586–608. https://doi.org/10.3390/network4040029

Academic Editor: Christos Bouras

Received: 20 October 2024
Revised: 25 November 2024
Accepted: 19 December 2024
Published: 21 December 2024

1. Introduction

Personal transportation has been a crucial means of travelling for humans for decades. However, with current petrol vehicles not being eco-friendly, as they pollute the air, the demand for greener transport, like electric vehicles (EVs), has increased. However, world institutions have not been able to drastically adopt EVs because the Li-ion batteries used in EVs are not fully stable and efficient, as the battery overheats and degrades over time from usage. The global demand for Li-ion batteries is increasing exceedingly, and it is expected to increase from the required 700 GWh in 2022 to around 4.7 TWh by 2030 [1]. Hence, research on technologies such as battery management systems (BMSs), which will play major role in meeting this market demand, has become a hot topic; this report evaluates these technologies. The main subject of this report is to design and build a BMS for EVs, a system that monitors battery condition and critical parameters, such as voltage (V), current (I), temperature (T), state of charge (SOC), and state of health (SOH), and alerts the end-user when the battery conditions are abnormal through a user-interface display [2,3]. Current challenges in the development of a BMS for electric vehicles include ensuring accurate estimation of battery states (SOC and SOH) under dynamic operational and environmental conditions, such as varying temperatures and load profiles. Additionally, balancing the computational demands of advanced algorithms with real-time constraints and maintaining cost-effectiveness while integrating features like the IoT and thermal management systems remain significant hurdles. This research addresses these challenges by developing a robust BMS that integrates UKF-based estimation for high precision, IoT-enabled remote monitoring for predictive maintenance and adaptive thermal management to enhance safety and efficiency. The findings aim to provide a scalable and practical solution for optimising EV battery performance and lifespan.

The main reason that BMS technology is relevant for the EV industry is it can improve the battery safety by monitoring and managing it so that it is not being overcharged or discharged. This also optimises battery usage and minimises energy loss, increasing the battery's reliability for giving a constant smooth high performance. This further leads to the battery having a longer life span, as its health degrades far slower, thereby reducing the cost of battery service and maintenance.

This paper aims to critically analyse and evaluate various existing BMSs to develop and simulate the most optimum BMS for EVs which is robust and adaptive at accurately estimating the battery's critical parameters in real-time and managing the battery for optimum performance by efficiently conserving battery energy and health throughout its operational life cycle. To achieve this, a comprehensive review of the literature was conducted on the scientific theories and methods that can be used to monitor and estimate battery parameters in BMSs, such as the traditional and modern estimation methods. A BMS simulation and physical model were created with an IoT-based user interface that consisted of an interface between the BMS simulation program and the Arduino board.

The relevant previously developed BMS is presented in [4], which consists of a BMS that has a load connected to a battery, being measured by an INA219 sensor for monitoring current and a MAX6675 sensor for measuring temperature. The INA219 sensor has range to measure a maximum of 26 V and 3.2 A. The MAX6675 sensor is a K-type thermocouple which can measure in a range from 0 to 1024 C. It has an ESP32 microcontroller which processes the sensors data and uses a coulomb counting method to calculate the SOC. The long range (LoRa) module is used for the wireless transmission of data to another LoRa, which then passes it to another ESP32, which then transfers the data to an OLED screen and on to an IoT cloud for data display. The LoRa module is a technology that allows communication through a wide area network (WAN), which is used to receive and send data from sensors through a wide area wirelessly. The LoRa sends its data through radio waves at a frequency of 869 MHz. Another wireless data transmission technology available is a Wi-Fi module, which allows for wireless communication using a Wi-Fi network.

Another slightly different developed BMS, illustrated in [5], consists of a BMS which has the battery being monitored by a voltage sensor and DHT11 sensor for measuring temperature. The voltage sensor uses a potential divider to measure voltage and has a range of a maximum of 25 V. The DHT11 sensor can measure to a range from -40 to 125 °C. It has an ATMEGA 328P microcontroller and uses a coulomb counting method for estimating the SOC. The data is directly transferred to an LCD and is also wirelessly transferred to an IoT cloud using MQTT which is a commonly used messaging protocol for communication between a machine and an IoT device. An IoT devices is an appliance or sensor that is capable of exchanging data by sending and receiving information wirelessly through a network, such as the internet; hence, it is interconnected. IoT is commonly used for monitoring data from sensors and remotely controlling the device. The cloud in the network, which supports the IoT, is the place where the transferred data is stored, processed and remotely viewed by the user.

The key contributions of this paper can be summarised as follows:

- Innovative integration of advanced estimation techniques: This paper introduces a novel BMS that integrates advanced KFs and other cutting-edge, data-driven estimation techniques, providing a more accurate and adaptable method for monitoring the state of a battery. This approach not only enhances precision across battery cycles but reduces the error margin significantly, demonstrating a marked improvement over traditional techniques.

- Real-time BMS implementation with IoT and Simulink integration: The proposed BMS uniquely combines real-time data processing through a Simulink model with physical implementation using an Arduino board and an IoT platform. This integration creates a robust and adaptive BMS capable of real-time battery management, offering a practical and scalable solution that bridges the gap between theoretical models and real-world applications.
- Comprehensive benchmarking and analytical comparison: The paper conducts an extensive benchmarking of traditional versus modern estimation techniques within the BMS context, offering a detailed analytical comparison. This evaluation not only highlights the effectiveness of advanced methods but provides a clear academic and practical framework for selecting the most appropriate techniques for different BMS applications.

The main motivation behind this research was to further critically analyse and enrich the available knowledge on BMSs, which can act as a catalyst to further accelerate the adoption of EVs in modern society and preserve our planet for future generations. Other reasons were to socially improve society's perception and acceptance of battery powered EVs by improving the safety of the battery during high stress conditions and operations commonly known for creating malfunctions and safety risks in the battery. This mitigates any personal risk or risks to the surrounding environment, like explosions or fire caused by the battery. This further enhances the safeguarding of public health and well-being and helps in promoting the transition to green energy by increasing the awareness and a social ideology shift towards the use of cleaner energy solutions, like battery powered EVs. Vast inspiration was taken from the current pioneers in this field paving the path, companies like Tesla, Mercedes, Toyota, and BYD.

2. Literature Review and Methodology

2.1. Relevant Theories

State of charge (SOC) is a performance parameter for a battery which indicates the amount of remaining charge left as well as the power level. When the SOC level is 100%, the battery is fully charged; when its 0%, it is fully discharged. In practical applications, however, the SOC level will range between 90% and 30% [6]. Equation (1) provides a basic estimate of the SOC [7].

$$\mathrm{SOC}\ (\%) = \frac{\mathrm{Q_{stored}}}{\mathrm{Q_{max}}} \times 100 \tag{1}$$

State of health (SOH) is another performance parameter for a battery which indicates the remaining capacity usable for the charging and discharging process. It also shows the level of degradation of the battery from the usage; this is shown in Equation (2). The initial SOH of battery is 100% but after 300 to 600 cycles, the SOH typically drops to between 60% and 70% due to battery degradation [6]. The SOH also indicates how long the battery's useful lifetime is by comparing the battery's present conditions to its initial manufacturing condition [8].

$$\mathrm{SOH}\ (\%) = \frac{\mathrm{Q_{max}}}{\mathrm{C_{rated}}} \times 100 \tag{2}$$

An equivalent circuit modelling (ECM) technique [9] is used to model and represent the dynamics of a Li-ion battery, to comprehend and simulate its complex behaviour. Figure 1 demonstrates the ECM of a battery. The ECM is essential for simulating batteries, providing real-time monitoring of key parameters and insights into internal behaviours like SOC and SOH. This makes it crucial for optimising battery performance and developing effective control protocols in a BMS [10].

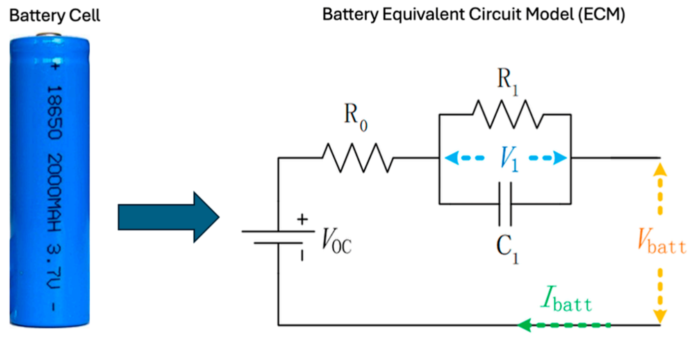

Figure 1. Equivalent Circuit Model of a Battery.

2.2. Affecting Factors

The charging and discharging process of the battery is a complex electrochemical process which is affected by various factors that prevent the accurate estimation of SOC and SOH values.

- Discharge rate: One of these factors is the rate at which the current is being discharged from the battery. When the discharge rate is high, it affects the battery capacity by reducing it and making the battery utilisation rate lower because the active material in the battery has a limited action that it can perform, thereby affecting the SOC and SOH [7].
- Battery temperature: Temperature affects the battery's power. As the temperature increases, the electrolytes in the battery become more active, which leads to battery utilisation rate and available power being increased. Whereas, when the temperature decreases, the electrolytes become less active which reduces the utilisation rate and power of the battery, thereby affecting the SOH. The ideal temperature range for a typical Li-ion battery to function effectively is between the range of 0 °C and 45 °C [7].
- Number of cycles: The amount of charging and discharging cycles that the battery has performed during its usage affects the battery's life. As the cycles increase, the total charge capacity of the battery decreases [7].

2.3. Traditional Estimation Methods

One traditional method to calculate SOC and SOH is the open-circuit voltage (OCV) method, which compares the battery's open-circuit voltage with a known OCV vs. SOC graph. However, the OCV method can be challenging to use for real-time application as it requires the battery to be rested for stabilisation before the method can be applied to it, which is not applicable as the Li-ion battery is a non-linear system which is prone to instability [11].

The coulomb counting (CC) estimates the SOC by integrating battery current over time. For example, 94 Ah corresponds to 100% SOC, 47 Ah to 50%, 23.5 Ah to 25%, and 0 Ah to 0% [12]. The CC method estimates the relative SOC by tracking current flow in and out of the battery, offering real-time and accurate calculations. However, it requires a known initial SOC and can accumulate errors from inaccurate current measurements, which can be mitigated with high-accuracy sensors, though this increases costs. Implementation of the CC method consists of using Equation (3), which consists of the sum of the previous known battery's SOC level, the battery's rated capacity (C_{rated}), and the integration of the measured battery current (I_b) which is entering or leaving the battery over a given time to calculate changes in the SOC level of the battery [13].

$$\mathrm{SOC} = \mathrm{SOC}(\mathrm{t}_0) + \frac{1}{\mathrm{C}_{\mathrm{rated}}} \int_0^{\mathrm{t}} \mathrm{I}_\mathrm{b}\,\mathrm{dt} \tag{3}$$

The internal resistance (IR) method consists of measuring the internal resistance of an Li-ion battery. The experiment consists of using a known value resistor, like a 10 ohms resistor that has 5-watt power consumption [14]. Then, measure the no-load voltage of the battery cell using a multi-meter. Then, measure the load voltage of the battery with the 10 ohms resistor connected. Then, measure the voltage drop between the no-load and load voltages of the battery to find the current internal resistance of battery. Issues can include unwanted extra resistance from wires used or the resistor being warmed up, which can affect the accuracy of measured voltage drop [14]. Equation (4) shows that the battery voltage equals the no-load voltage multiplied by the load resistor (R) and total resistance. Using this principle, the internal resistance (r), a component of the total resistance, can be calculated by rearranging the Equation [15].

$$V_{loaded} = V_{no\_load}\left(\frac{R}{R + r}\right) \tag{4}$$

It is essential to find the internal resistance ($R_{b,k}$) of the battery to estimate the SOH, which is expressed in Equation (5). It compares the known resistance, such as the end-of-life resistance (R_{EoL}) and the initial internal resistance (R_{fresh}), with the measured battery's internal resistance ($R_{b,k}$) to obtain the SOH of the battery [16].

$$SOH_{b,k} = \frac{R_{EoL} - R_{b,k}}{R_{EoL} - R_{fresh}} \tag{5}$$

2.4. Modern Estimation Methods

The Kalman filter (KF) is an estimation algorithm that observes state variables that are not directly measurable. It uses a state transition model and measurement data to estimate the system state (x_k) and its uncertainty (P_k). By combining past observations with current sensor data, the KF produces a more accurate state estimate, filtering out noise. As a recursive filter, the KF repeatedly refines its estimates using previous states and input–output data, making it effective for systems with linear dynamics [7].

Figure 2 illustrates how the extension KF (EKF) estimates the system state (x_k) in four stages: initialisation, prediction, measurement, and update. In the initialisation stage, the previous state ($x_{k-1|k-1}$) and uncertainty ($P_{k-1|k-1}$) are established. The system's dynamics are defined using state–space equations, incorporating parameters like SOC and internal resistance (R0). As the EKF progresses, it updates the system state and increments the time step (k) for tracking the current estimate [17].

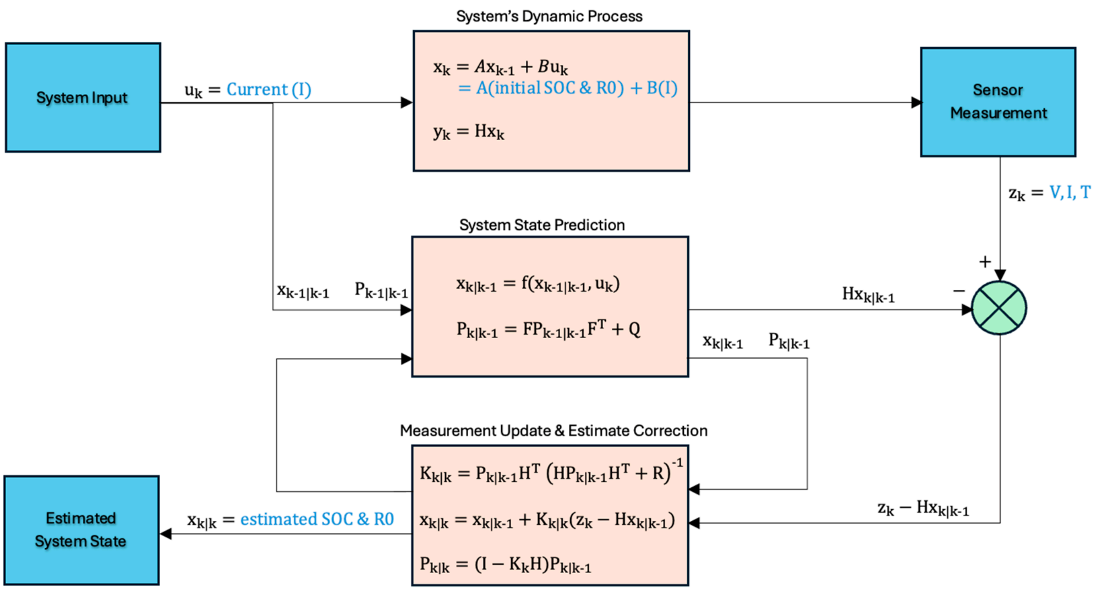

Figure 2. EKF Method Block Diagram.

The EKF operates in two main stages: prediction and update. In the prediction stage, the initial battery state and system input–output are used to predict the system state ($x_{k|k-1}$) and uncertainty ($P_{k-1|k-1}$). Since the models are non-linear, the Jacobian matrix (F) is computed for linearisation. The process also accounts for process noise (Q) and observed noise covariance (R) to enhance accuracy [18]. To minimise power consumption, the Kalman filters are configured to run intermittently based on predefined triggers, such as significant changes in battery parameters, rather than continuously. Additionally, the algorithms have been computationally optimised using efficient operations to reduce the processing burden on the BMS hardware. In addition, to address concerns about potential delays in real-time performance, the Kalman filters are implemented with computational optimisations to ensure minimal latency (in the range of milliseconds). Buffer mechanisms and threshold-based triggers are incorporated to prioritise critical actions, ensuring immediate responses when necessary.

In the update stage, the predicted state and covariance are adjusted using Kalman gain and sensor measurements (z_k) to improve accuracy. Kalman gain determines the balance between the model prediction and measurement data, with a higher gain favouring measurements. The final step extracts key elements, like SOC and R0, from the updated state ($x_{k|k-1}$), which are then used to calculate the SOH [8].

The EKF method Simulink model consists of using input battery parameters, like cell voltage, current, temperature, initial SOC, and initial R0. It uses a Jacobian matrix for linearisation, which is a matrix of all the first-order partial derivatives of a multivariate function or vector-valued function, to demonstrate the transformation of coordinates. It represents the linear transformation of a non-linear function by zooming into a specific point of the non-linear function and by looking at the linear relationship of the non-linear function. The Jacobian matrix (F) defines the state transition model matrix, and the Jacobian matrix (H) defines the observation transition model matrix of the EKF method which are linearised using Jacobians. After linearisation, it predicts the system state and error covariance, then it updates and corrects the estimated system state and it outputs the estimated system state from which the SOC and R0 levels are extracted as the estimated output battery parameters. The Simulink model of the UKF method is an alternative to EKF that can also be used to calculate the SOC. The UKF has the same objectives and system model as the EKF method, such as a prediction step and an update step, but the only difference is the method used for approaching the non-linear system which, for linearisation, uses sigma points. Then, the unscented transformation approach is used, which selects a set of sigma points (X) which are near the current state ($\hat{x}$). The unscented transformation is the approach to use probability distribution to calculate a random variable data which undergoes non-linear transformation. While the Jacobian uses a single specific point of the non-linear function to find its linear relationship, the sigma points use multiple points to find the non-linear function linear relationship [7,19]. To address potential inaccuracies in sensor data, the proposed BMS incorporates several error mitigation strategies. Sensor fusion techniques are employed to combine inputs from multiple sensors, cross-validating data and filtering out inconsistencies. Additionally, the Kalman filter's process and measurement noise covariance matrices are carefully tuned to model typical sensor inaccuracies and random noise effectively. These measures enhance the robustness of the SOC and SOH estimations. Diagnostic algorithms are also implemented to detect anomalies in sensor readings, triggering recalibration or switching to simpler estimation methods, such as Coulomb counting, when needed.

2.5. Proposed BMS Block Diagrams

Figure 3 outlines the six-stage structure of the BMS designed for this study, focused on ensuring proper battery safety and handling.

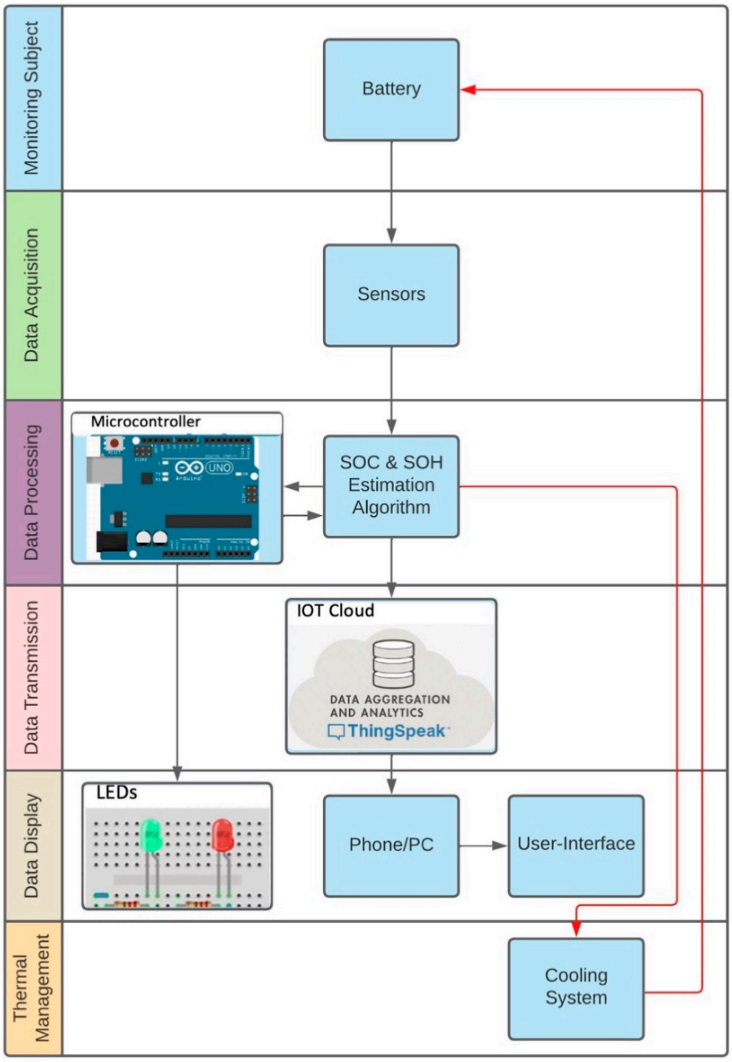

Figure 3. System Stages Block Diagram.

(1) Monitoring Stage:
- Component: Lithium-ion (Li-ion) Cell
- Function: Serves as the battery for the project.
- Reason for Use: EV batteries operate at high voltages (600–800 V), which are unsuitable for laboratory settings, whereas the Li-ion cell operates within a safe voltage range (3–4 V), making it suitable for lab work.

(2) Data Acquisition:
- Component: Dedicated sensors
- Function: Monitor and collect essential battery parameters required for estimating SOC (state of charge) and SOH (state of health).

(3) Data Processing:
- Component: SOC and SOH estimation algorithms, Arduino Uno
- Function: Execute the estimation algorithms to calculate the SOC and SOH levels and facilitate communication between the algorithms and the hardware.

(4) Data Transmission:
- Component: IoT cloud platform (ThingSpeak)
- Function: Transmit processed battery data through a Wi-Fi network for remote monitoring and data aggregation.

(5) Data Display:
- Component: User interface (UI), LED indicators
- Function: Display battery data on devices like phones or PCs. LED indicators provide visual alerts: Red LED for overheating; Green LED for normal temperature.

(6) Thermal Management:
- Component: Smart cooling system
- Function: Automatically activates when the battery temperature exceeds safe operational limits, maintaining the battery temperature within a safe range. The BMS is designed to maintain stable operations in real-world scenarios through its integrated thermal management system, which dynamically regulates battery temperature, and reinforced hardware to withstand environmental stresses, such as vibrations. Adaptive SOC and SOH estimation algorithms further ensure consistent performance under variable charging conditions.

Figure 4 illustrates the block diagram of the SOC and SOH estimation method within the BMS. At the core is a battery model developed based on an ECM to represent typical Li-ion battery behaviour. The current profile provides input to the SOC estimation algorithm, guiding the expected charging and discharging cycles of the battery. Dedicated sensors are employed to monitor and measure the critical operating conditions of the battery, including cell current, voltage, and temperature. These sensor readings are essential inputs for the SOC estimator. Additionally, the SOC estimator requires initial conditions, such as the initial SOC and internal resistance (R0) of the battery, for accurate calibration and estimation of the SOC. The SOC estimation is performed using multiple algorithms, including CC, EKF, and UKF, each contributing to the accuracy of the estimated SOC. The SOH estimator uses the estimated SOC and internal resistance (R0) to calculate the SOH of the battery. Finally, the system outputs the real SOC, estimated SOC, SOH, and internal resistance (R0) to the end-user, providing comprehensive information on the battery's current state.

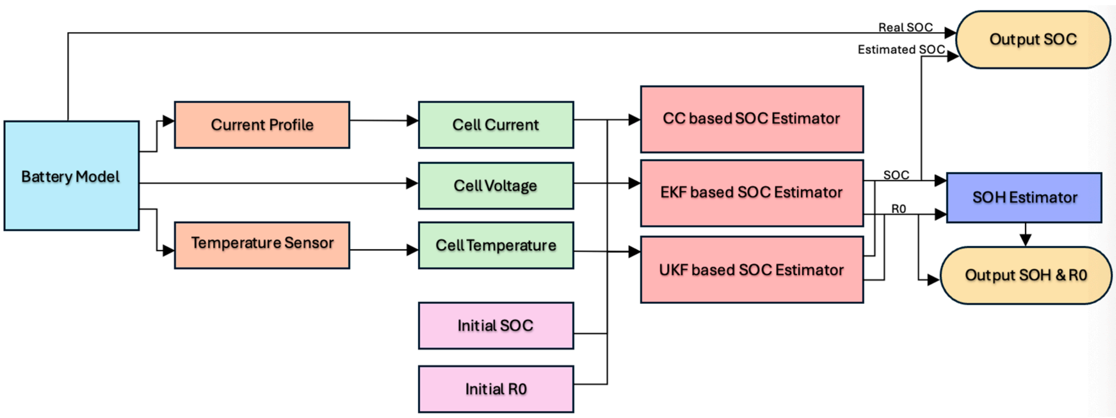

Figure 4. SOC and SOH Estimation Block Diagram.

2.6. Simulation and Practical BMS Model Implementation

Figure 5a demonstrates the simulation model of the BMS which is built using Simulink software version R2024a. The developed BMS consists of a battery model which is based on the ECM, the battery is set up to produce ten charging and discharging cycles, one full cycle per 1 h. The battery provides an output voltage range from 3.6 V to 4.2 V, a current of 15 Amps, and produces a temperature ranging from 295 to 336 K. The initial conditions of the battery have the SOC level at 30% and the R0 at 0.008 ohms, which can be seen in Table 1. Dedicated sensors, like voltage, current and temperature sensors, are used to monitor and measure the battery parameters. Random white noise is added together with the measured sensor values to make the measured battery parameters as realistic as possible to a real environment. Random noise will be introduced in the sensor measurements. Temperature fluctuations are simulated by introducing controlled ramps and random noise variations to emulate realistic environmental conditions. These variations cover a range of operating temperatures (295–336 K), reflecting typical scenarios, such as ambient cooling and heating effects, during charging and discharging cycles. Three SOC estimator algorithms are used, each algorithm assigned to a different estimation method, such as the first SOC estimator using the CC method, the second SOC estimator using the EKF method, and the third SOC estimator using the UKF method. The measurement of the battery parameters, such as voltage, current, and temperature, are the essential input parameters for the SOC estimator algorithms to function properly, and the estimated battery parameters output are the current SOC level and the internal resistance (R0) of battery. Whereas the initial SOC level given to the SOC estimators is 35%, and this is given to make it realistic, in a real environment the BMS will not know the exact initial SOC level of the battery, but it makes a guess; hence, there being slight initial inaccuracy. Two SOH estimator algorithms were also used, the first SOH estimator using the EKF method and the second SOC using the UKF method. The SOH estimator algorithm uses the outputs of the SOC estimators and battery temperature as their input parameters to calculate the SOH level of the battery. Digital display scopes are used to display the battery's parameters, like the real and estimated SOC levels, the estimated SOH levels, estimated R0, and the measured battery temperature. The BMS simulation model is designed to run in synchronisation to real-time by using the device's digital clock; hence the battery completes 5 charging and discharging cycles in 10 h [20,21].

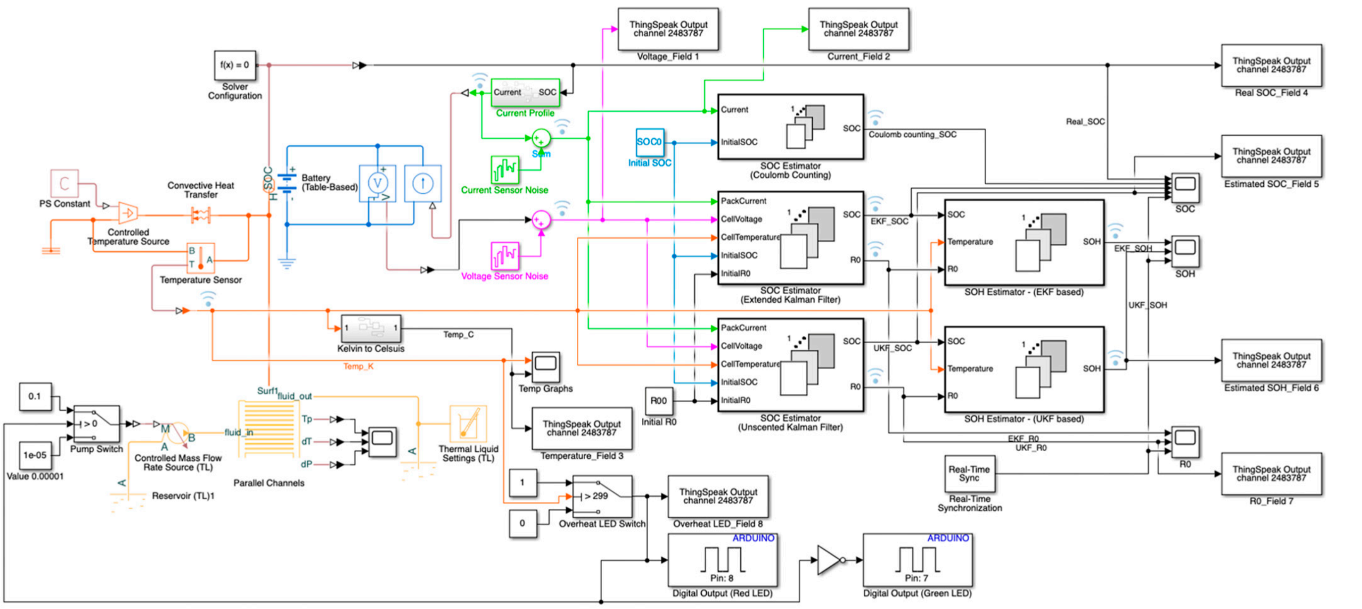

(a)

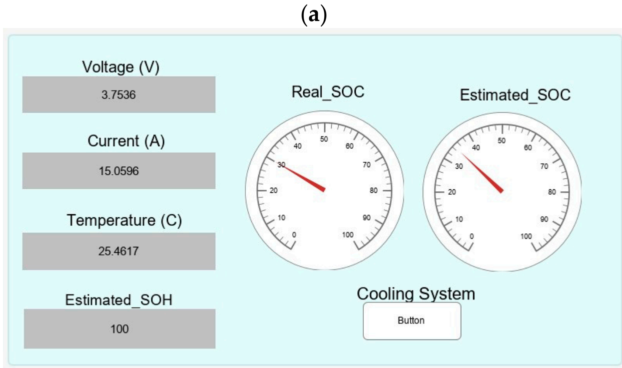

(b)

Figure 5. BMS Model (**a**) and User-interface (**b**) for BMS Simulation Simulink Model Implementation.

Table 1. Initial parameter setting table of the battery and BMS.

Parameter	Value
Current	15 Amps
Temperature	295 to 336 K
Initial SOC of battery	30%
Initial SOC given to SOC estimator	35%
Initial R0 of battery and given to SOC estimator	0.0008 ohms
Sensor Noise	Random white noise
Battery Cycle Time	1 complete charging and discharging cycle per hour
Number of Completed Battery Cycles	5 cycles completed in 10 h

Battery thermal management is essential for maintaining safe and efficient battery operations, and the developed BMS does this by regulating the battery temperature at regular intervals using a smart cooling system that has been added to the BMS. The cooling system is based on a passive cooling solution which consists of using a parallel channel cooling plate connected to the battery's thermal source, a reservoir thermal liquid and a pump used for pumping the thermal liquid throughout the pipes or channels in the cooling plate, and a switch for turning on and off the pump. The battery cooling plate has a pair of distributor channels for inlet and outlet flow of the thermal liquid. The cooling system uses the temperature sensor's measurements to track the battery temperature in comparison to the assigned safe operating temperature limit, which is 299 Kelvin; when the battery exceeds this limit, the switch automatically turns on the pump which increases the amount of thermal liquid being pumped in the cooling plate, this leads to more heat being extracted and transferred from the battery through the thermal liquid circulation inside the cooling plate that channels near the battery cell, which drops the battery temperature into a safe temperature range below 299 K. Conversion from Kelvin to Celsius was also performed, which displays temperature in range from 25 to 36 °C. To alert the end-user when the battery is overheating, two LEDs connected to the Arduino board with a switch are used. The switch is assigned a temperature threshold; when this limit is exceeded, a signal of "1", which is read as "high", is sent to the Arduino board's output digital pin 8 which then turns on the red LED connected to it and an inverter (NOT logic gate) is used to convert the "1" signal to "0". This turns off the green LED which is connected to the Arduino's output digital pin 7. This process happens vice-versa when the temperature drops below the assigned threshold. For establishing the connection and interface between the Simulink model and the Arduino board, Simulink's hardware support library is used. To transmit data to the IoT "ThingSpeak" platform, the Simulink model uses the in-built ThingSpeak connecting function block and the device's Wi-Fi module to connect to the IoT cloud. The ThingSpeak function block uses the ID details of the created user interface on the ThingSpeak platform such as its channel ID "2483787", which is unique to each created channel, the API key, which is the writing key needed to access and write in this channel, and the field number, which informs in which block or display the channel needs to be written in. A user interface was also created in the Simulink model shown in Figure 5b to allow the end-user to interact and manage the BMS in the Simulink software. It consists of displays that show the measured and estimated battery parameters in LCD and gauge display formats; it also has a manual button for turning on the cooling system [20,21].

Figure 6 demonstrates the setup used to implement and verify the SOC and SOH estimation algorithms in the BMS by having the BMS's Simulink simulation program running in one computer on the left side and having the IoT platform user interface running on the second computer on the right side. It also shows the interface occurring between the Simulink program and the hardware "Arduino Uno board" that is connected to two LEDs on the left side, which shows the green LED being turned on, hence informing the end-user that the battery is operating under normal and in the safe temperature range. The IoT platform displays the up-to-date updates of the new measured and estimated parameters of the battery at regular intervals of 15 s from the Simulink program to the IoT in the form of plot graphs, numerical displays, and gauge displays for the end-user on their computer in a user-friendly manner.

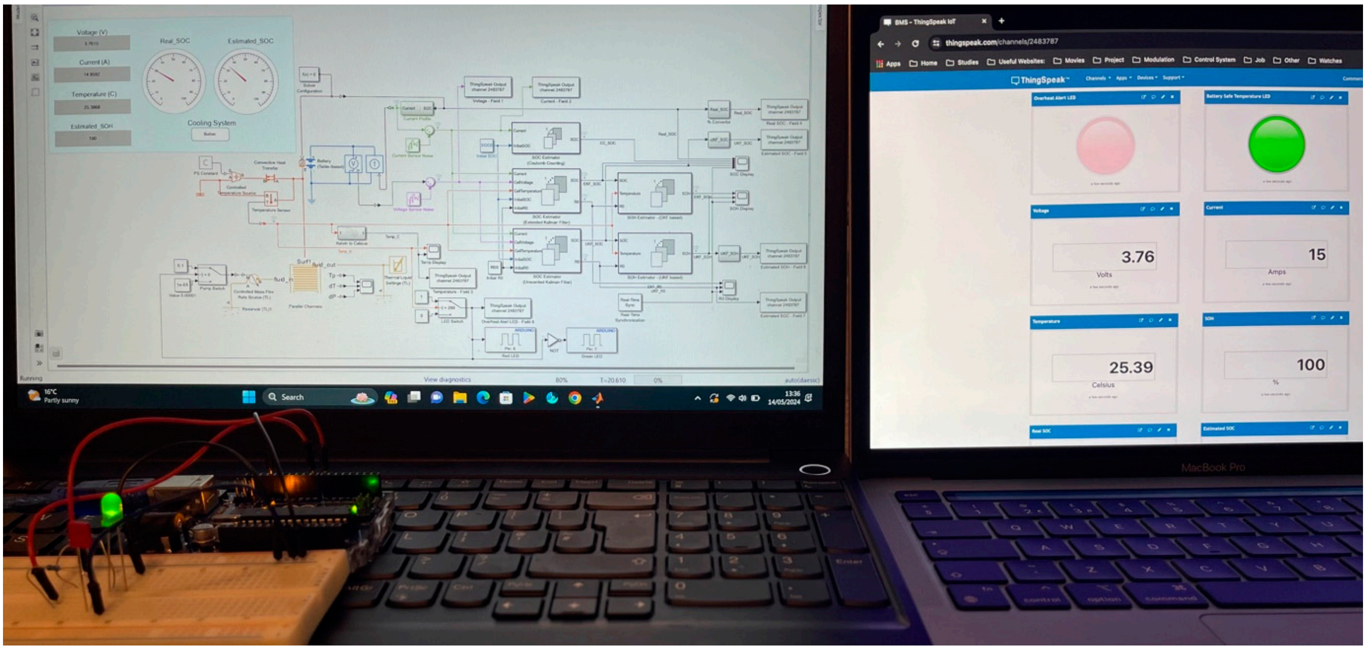

Figure 6. Practical BMS Model Implementation.

3. Results

Figure 7 shows the graphs of the measured battery parameters using the dedicated sensors, such as voltage and current. Its shows that, when the battery is charging, it ranges from 3.7 V to a maximum voltage of 4.3 V; when the battery is discharging, it ranges from 4.3 V to 2.9 V. When the battery is charging the maximum current being supplied is 15 Amps.

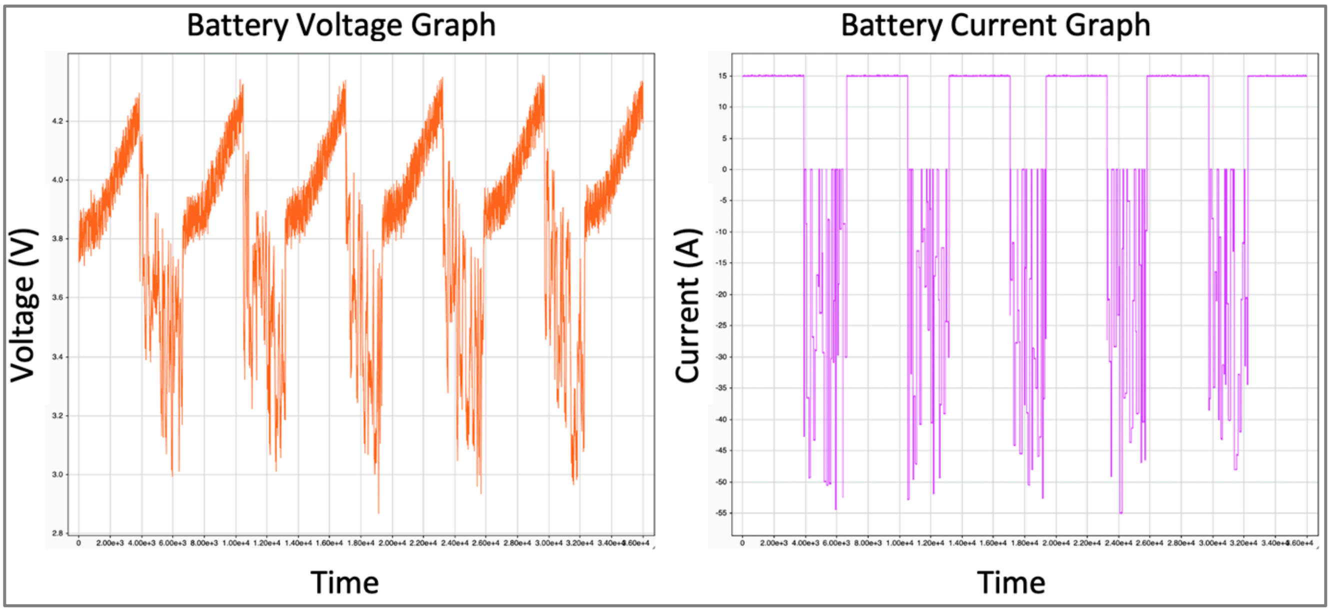

Figure 7. Measured Voltage and Current Graphs.

Figure 8 demonstrates the battery's calculated SOC graphs, which consists of the measured real SOC and the estimated SOC graphs of the battery. The real SOC is the yellow-coloured graph; the CC method-based estimated SOC is the blue-coloured graph; the EKF method-based estimated SOC is the red-coloured graph; and the UKF method-based estimated SOC is the green-coloured graph. The real SOC graph starts plotting the battery charging graph from 0.30 which, in the percentage format, is 30 precent, and it goes up to 90%, at which point the battery is fully charged. Whereas the battery discharging graph goes from 90% to 30%, at which point the battery is fully discharged. The battery repeats this charging and discharging cycle for five cycles. It also shows that the estimated SOC graphs are trying to track and follow the real SOC graph. It is evidently presented from the results that the SOC estimation method which achieved the worst results in accurately tracking the real SOC graph is the CC method; the method which was most accurate at tracking the real SOC is the UKF method, which can be seen by the green-coloured UKF-based SOC graph overlapping the yellow-coloured real SOC graph. The EKF-based SOC graph is also giving very accurate results, but it can also be seen that it has some unwanted spikes that appear at some places in the red-coloured SOC graph, due to errors or disturbances in the system. Figure 9 presents the zoomed-in graph of Figure 8 that focuses on only the first and second cycles of the battery for a closer look at the battery SOC graph and to obtain a better understanding of the battery dynamics.

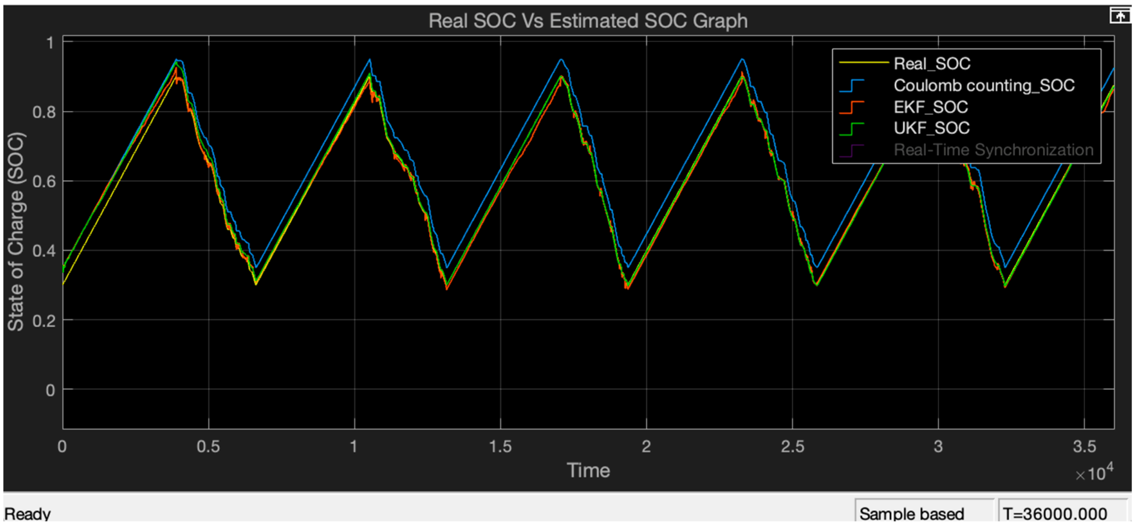

Figure 8. Real and Estimated SOC Graphs.

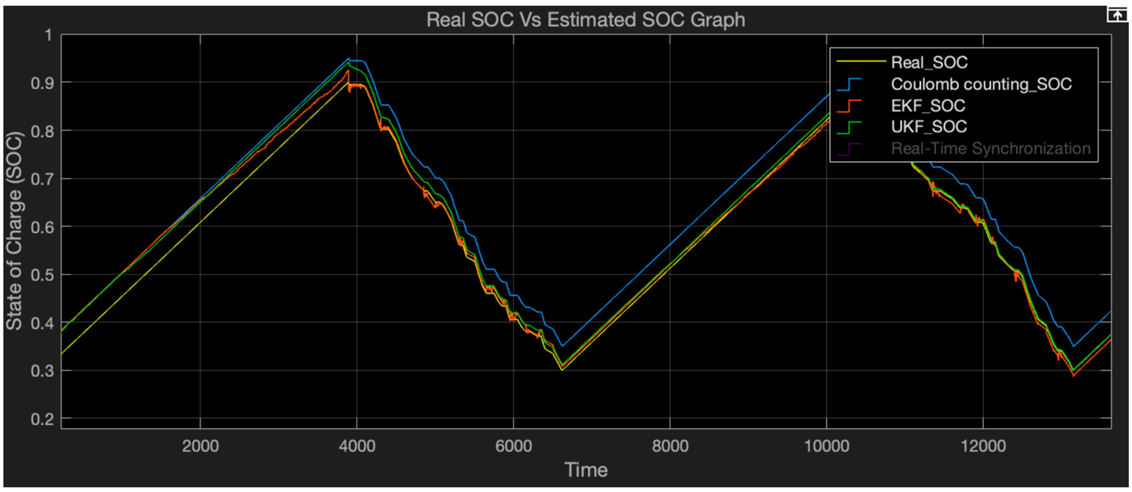

Figure 9. Zoomed SOC Graph.

Figure 10 presents the battery's estimated state of health (SOH) graphs, which consists of the estimated SOH based on the EKF method that is the yellow-coloured graph, and the estimated SOH based on the UKF method which is the blue-coloured graph. The plotting of the SOH graph starts from 1 which, in the percentage format, is 100%; hence, the battery being fully healthy, which means it is basically a brand new battery. Then, as the time increases while the battery performs multiple charging and discharging cycles, the battery's SOH level starts to decrease causing battery degradation from the excessive usage such that the SOH level drops between the range of 70% and 80%. It also shows that the UKF-based SOH estimation graph is smoother and more accurate as it narrows the SOH level range to as close to the real SOH of the battery. While the EKF-based SOH estimation graph is more widespread and covers a large range and fluctuates a lot, thus being less accurate than the UKF-based SOH graph and being just a rough estimate of the battery's SOH level.

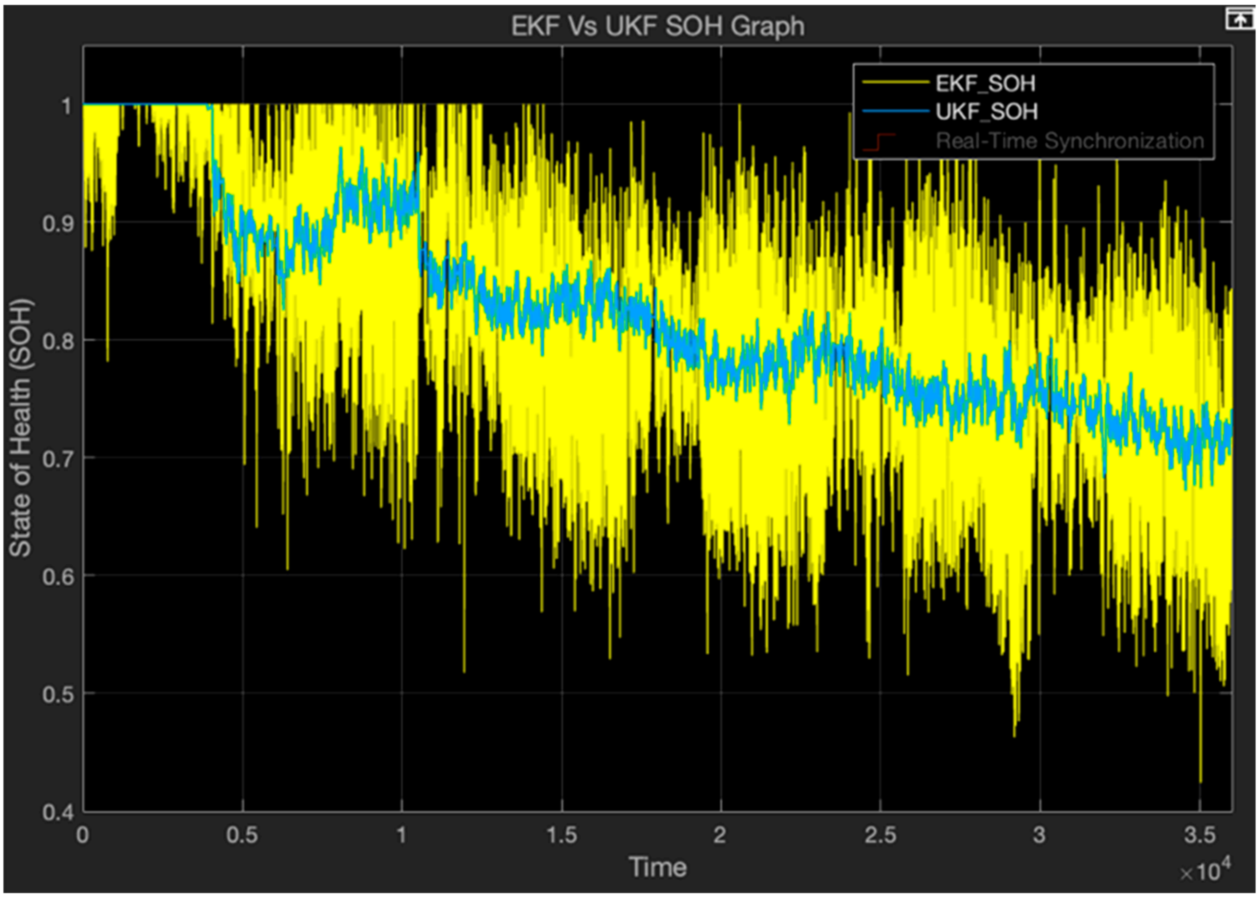

Figure 10. Estimated SOH Graphs.

Figure 11 demonstrates the battery's estimated internal resistance (R0) graphs, which consists of the estimated R0 based on the EKF method, which is the yellow-coloured graph, and the estimated R0 based on the UKF method, which is the blue-coloured graph. The plotting of the R0 graph starts from 0.008 ohms resistance, which represents the initial resistance of the battery. Then, as the time increases while the battery executes multiple cycles, the battery's R0 level starts to increase from battery usage along with an increase in the battery temperature to the R0 level being between the range of 0.010 and 0.015 ohms resistance. It also shows that the UKF-based SOH estimation graph is smoother and more accurate, while the EKF-based R0 estimation graph is fluctuating more and is less accurate then UKF-based R0 graph.

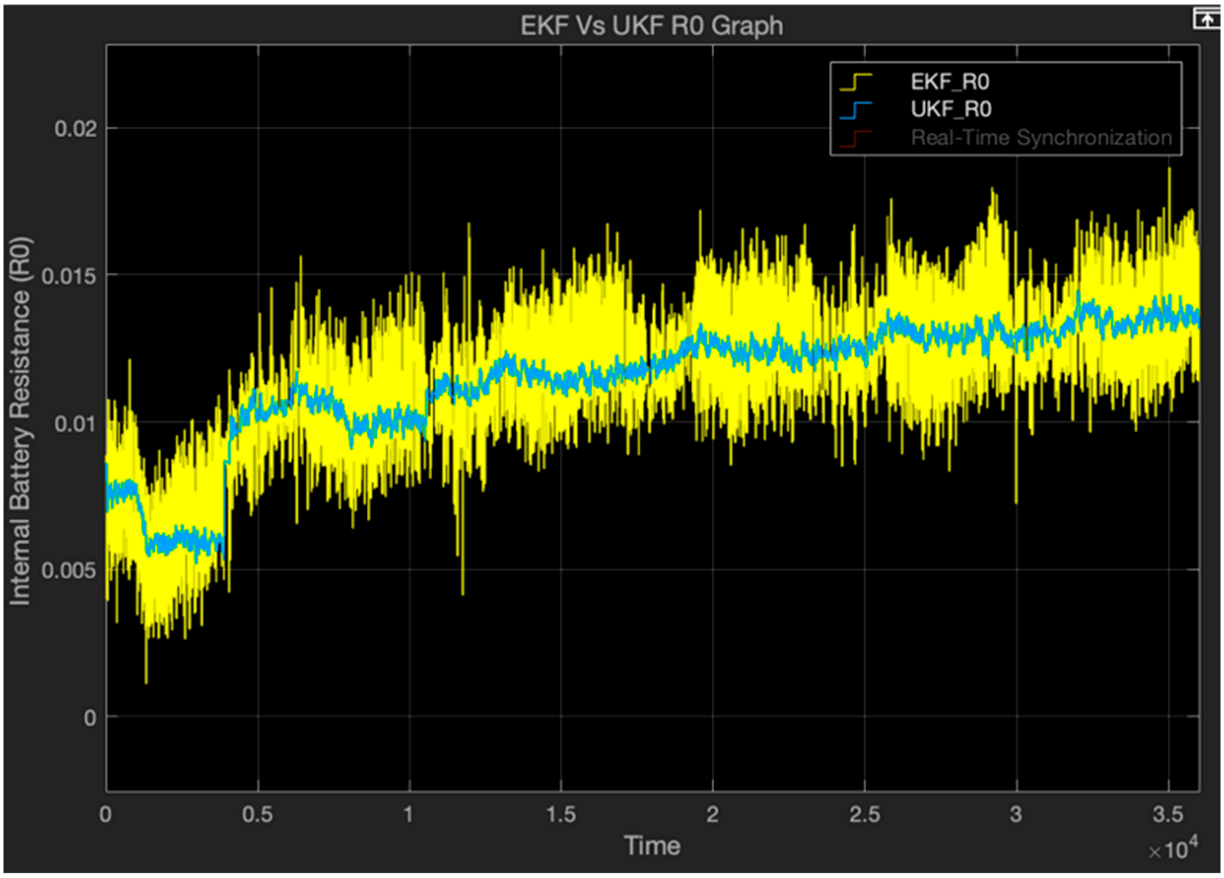

Figure 11. Estimated R0 Graphs.

Figure 12a presents the battery's measured temperature graph with no cooling system turned on, in the Kelvin unit (K), which is the top graph, and in the Celsius unit (C), which is the bottom graph. The Kelvin unit was used because the SOC estimators required it to function properly; the Celsius unit was used because it is the most common temperature unit used by the public. Hence, it is for the user to read. The graphs show that, as the number battery cycles completed increases by time, so does the battery temperature increase. Temperature increased from 298 K to 308 K or from 24 °C to 34 °C.

Figure 12b illustrates the battery's measured temperature graph with the cooling system turned on. It shows that, as the battery temperature reached 299 K or 25.8 C, the cooling system turns on automatically, which drops the battery temperature and prevents it from exceeding the assigned limit of 299 K or 28 °C, hence the battery's cooling system is operating exceptionally at keeping the battery operating safely.

Figure 13a,b displays the transmitted battery parameters on the IoT "ThingSpeak" platform in the visualised format such as the LEDs indictor which shows the green LED being turned on, indicating that the battery is operating safely. The platform uses the LCD display to display the measured battery voltage of 3.82 V, current of 15 Amps, temperature of 26.75 °C, and the SOH level of 100% as its first cycle to indicate the battery is brand new; the real SOC level is approximately 30% and the estimated SOC is 35% because the initially given SOC level to the SOC estimator is 35%. Hence, in start estimations, there is a slight error but the BMS will adjust to more accuracy with more battery cycles; the internal resistance of 0.008 ohms is also measured.

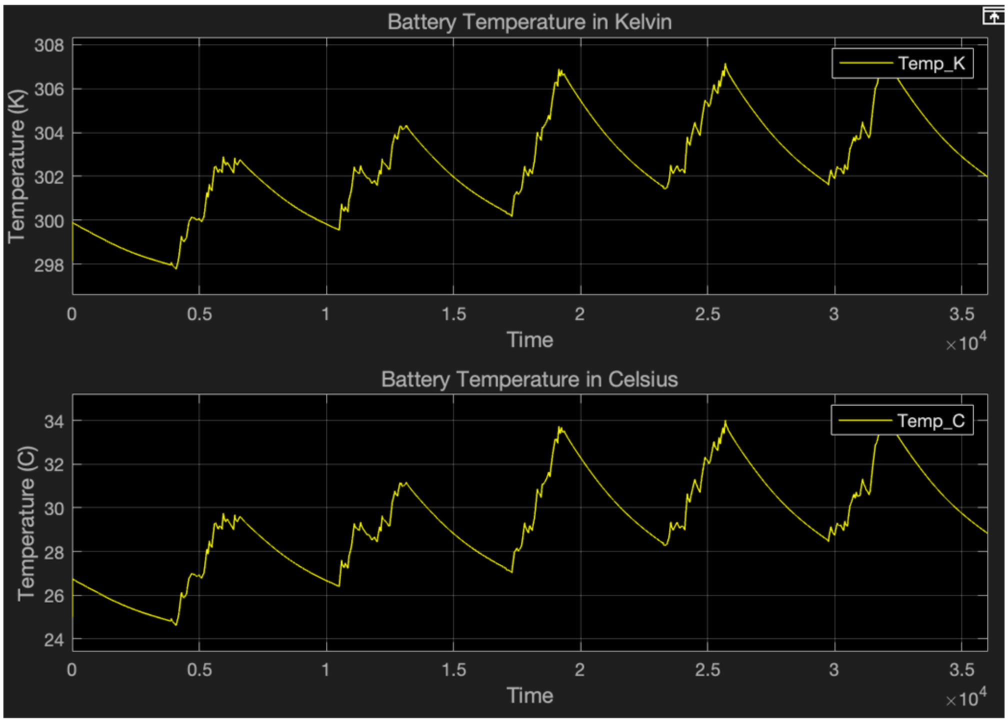

(**a**)

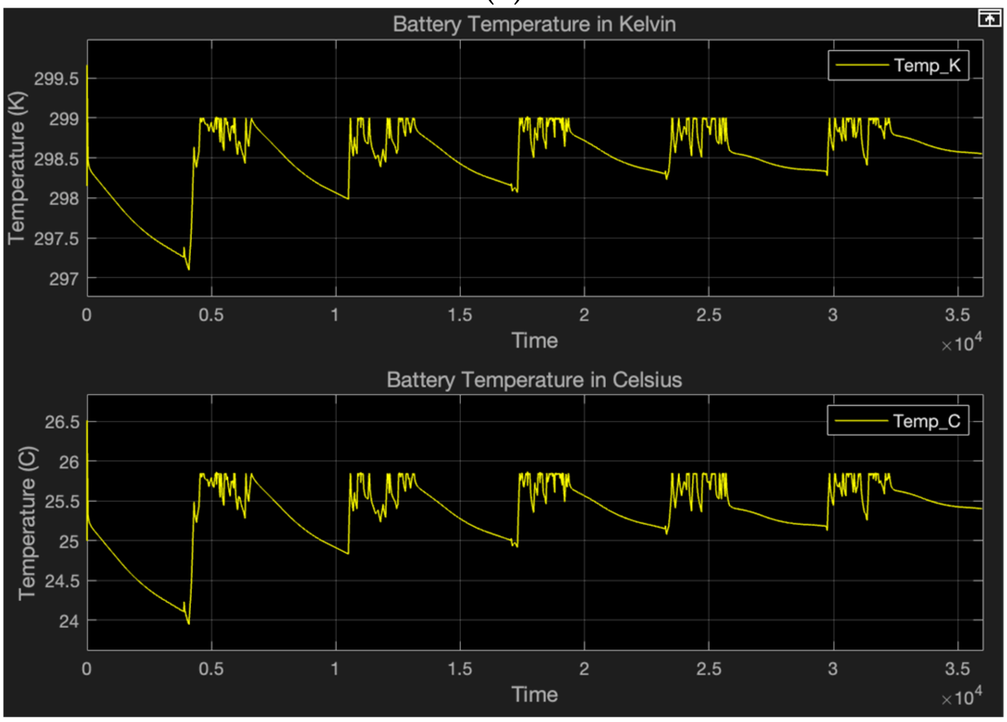

(**b**)

Figure 12. (**a**) Show Measured Temperature Graphs with Cooling and (**b**) without Cooling.

Figure 14 presents the BMS's battery overheating alert indicator system functioning properly, which can be seen as the battery is overheating: the red LED has been turned on and the green LED has been turned off, which informs and alert the end-user of the battery overheating status. Even the battery overheat alert LED graph shows a spike of value being 1 when red LED is turned on.

(**a**)

(**b**)

Figure 13. (**a**,**b**) Show Battery Parameters Displayed on IoT Platform.

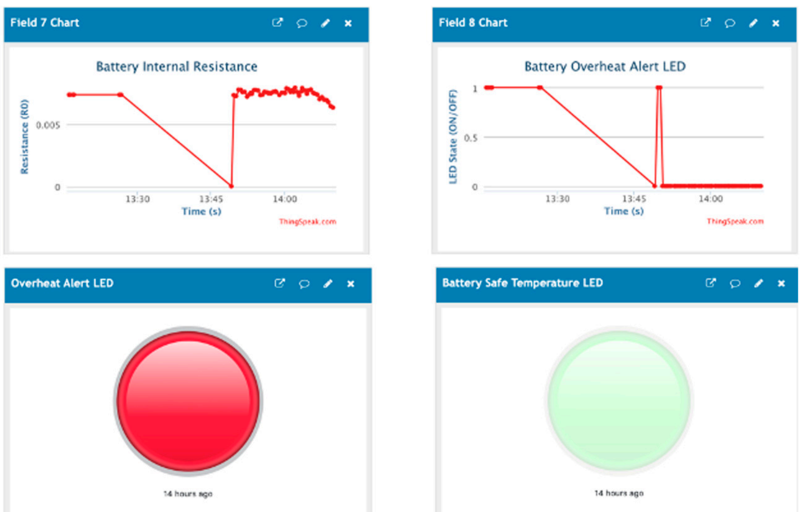

Figure 14. Red LED Turning on When Battery Overheating.

4. Discussion

Aspects of the BMS which were analysed are the SOH, the battery temperature, the efficiency of the BMS performance, and the error margin of the BMS at tracking the real SOC level. Further investigation of the battery's estimated SOH graph, as shown in Figure 10, has revealed a relationship of SOH level drop over time which is shown that in the initial time from 0 to 2000 s, the drop in the SOH is significantly high; but in the later time, from 2000 s to 3500 s, the SOH drop reduces excessively. The SOH at time 0 s is 100%; the SOH at time 500 s is 90%; the SOH at time 1000 s is 87%; the SOH at time 1500 s is 85%; the SOH at time 2000 s is 78%; the SOH at time 2500 s is 77%; the SOH at time 3000 s is 76%; and the SOH at time 3500 s is 75%. This is because, at the initial time, the battery must undergo a conditioning phase in order to stabilise the internal chemical process, this adds a sufficiently high level of stress on the battery which increases the battery degradation, hence reducing the SOH level faster [22,23]. Whereas, in the later period of the battery after some cycles, the battery's internal components are stabilised, providing a consistent performance with a slower battery degradation rate thereby reducing the SOH level slower.

Inspection of the battery's measured temperature graph, which is presented in Figure 12a, has demonstrated the pattern of the battery temperature dropping when the battery is charging; when the battery is discharging, the battery temperature increases. It also shows that, as the number of discharge cycles of battery increases, so does the battery's temperature increase significantly. The reason for this is that, during the charging process, the battery tends to store electrical energy by converting its internal chemical energy into stored electrical energy through electrochemical reactions, and these reactions by nature tend to be endothermic, which means that they absorb the heat from the surroundings; and the charging process, with it ions migrating and redistributing, can also introduce a cooling effect on the battery. All these effects led to the battery temperature dropping [24,25]. During the discharging process, the battery's chemical energy is converted to electrical energy and this process involves exothermic electrochemical reactions, which means that the battery releases heat in its surroundings, thereby increasing the battery temperature. Further utilising this information, it is possible to improve the BMS performance by enhancing the battery cooling system through creating better thermal management strategies and protocols by specifically considering and tackling the cooling of the battery during its discharge cycle period for a more robust and effective cooling response on the battery in a more energy efficient way.

The BMS efficiency at tracking and estimating the SOC level at the conducted five charging and discharging cycles of the battery under the BMS management shows that the first battery cycle SOC estimation graph does start with a slightly higher error margin, but that is understandable as the input initial SOC level condition to the SOC estimators is fully accurate, hence the BMS takes a bit of time to adjust; however, from the second to fifth battery cycles, it is shown to provide an average of 90% SOC for a fully charged battery; for a fully discharged battery, it provides a 30% SOC level, which is identical to the real SOC levels measured. Hence, the BMS proves its high efficiency in providing a constant smooth performance and energy transfer, which is also evident from the minor error margins presented in Table 2. The proposed BMS achieves a balance between computational complexity and energy efficiency by selectively processing data. Power consumption measurements indicate that the energy used by the BMS for running advanced algorithms is negligible compared to the improvements in battery performance achieved through accurate SOC and SOH estimations.

During analysis it is also seen in Figure 8 that, during the battery discharge, the SOC graphs are rougher and have more fluctuations compared to when battery is charging, which smoother. The reason for this is that, during the charging process, the battery's electrochemical reactions are controllable and predictable and even the charging current to the battery is supplied externally, which can also be precisely controlled; hence, the battery having a smooth SOC level increase during charging. Whereas, during the discharging process, the battery is the one providing the discharge current from its internally stored energy and this discharge process can be affected by factors, like varying load resistance being introduced to the battery, introduced random white noise, changing internal resistance, and battery conditions, which could lead to a rough SOC level graph during battery discharge [23,25].

Table 2. Comparison of real and estimated SOC levels with various estimation techniques.

	Battery Charging					Battery Discharging					Average Error Margin	
Cycles	1st	2nd	3rd	4th	5th	1st	2nd	3rd	4th	5th	Charge	Discharge
Real Value	90%	90	90	90	90	30	30	30	30	30		
Estimated CC	95%	95	95	95	95	35	35	35	35	35	5%	5%
Estimated EKF	92%	89	89	88	92	31	29	29	29	29	1.6%	1%
Estimated UKF	94%	91	90	90	90	31.5	30	30	30	29.9	1%	0.32%
CC Error Margin	5%	5	5	5	5	5	5	5	5	5		
EKF Error Margin	2%	1	1	2	2	1	1	1	1	1		
UKF Error Margin	4%	1	0	0	0	1.5	0	0	0	0.1		

The system's robustness to noisy sensor data is demonstrated by the UKF's low error margins, even under simulated inaccuracies. Noise modelling and covariance tuning in the Kalman filters ensured reliable SOC and SOH estimations, maintaining error margins as low as 0.32% during discharge cycles despite the introduced noise.

Table 2 shows the comparison of results of the battery's measured real SOC level vs. the estimated SOC levels based on the CC, EKF and UKF methods. The error margin is calculated, which informs by how much the estimated SOC levels diverge from the real SOC measured; this is performed to find the most accurate SOC estimation method: it shows the SOC levels measured over five battery charging and discharging cycles. The average calculated error margin for the CC-based SOC is 5%, for the EKF-based SOC is between 1.6% and 1%, and for the UKF-based SOC is between 1% and 0.32%, which is the lowest. The SOC estimation performance of the proposed BMS was evaluated against industry standards, such as IEC 62660-2 and ISO 12405-4, which specify acceptable error margins for the SOC tracking in electric vehicle applications. These standards typically set thresholds around 1–2% error for advanced systems. The results of this study, with error margins ranging from 0.32% to 1%, demonstrate compliance with and surpass these guidelines, emphasising the robustness and accuracy of the proposed approach. Testing under simulated real-time conditions has shown that the delay introduced by the Kalman filters is negligible for typical EV operations. The system's design prioritises critical actions, such as thermal management and fault detection, over non-critical SOC and SOH updates, ensuring responsiveness in high-demand scenarios.

Table 3 presents the comparison of results of the battery's real SOC vs. estimated SOC levels, when different initial SOC levels are given as the initial condition to the SOC estimators. At 40%, the initial SOC level given, the average calculated error margin for the CC-based SOC is 10%; for the EKF, it is between 2.7% and 1%; and for UKF, it is between 1.68% and 0.7%. Whereas, at the 50% initial SOC level, the average calculated error margin for the CC-based SOC is 20%; for the EKF, it is between 4.8% and 0.8%; and for the UKF, it is between 2.4% and 1.8%.

This shows that, as inaccuracy of the BMS's SOC estimators is increased purposely to test how the estimator algorithms react to it, the modern methods which are the EKF and UKF methods have proven to be more resilient, adaptive, and robust at minimising the error margin and more accurate at the SOC and SOH estimations. Whereas the traditional method, which is the CC method, has shown to be less accurate and adaptive to this system initial condition changes, which can be seen by the significantly excessive increase in the error margins of SOC estimation; as the SOC estimation worsens, so does the SOH estimation accuracy drop.

Table 3. Comparison of real and estimated SOC levels with different initial SOC conditions.

		Battery Charging					Battery Discharging					Error Margin	
Cycles		1st	2nd	3rd	4th	5th	1st	2nd	3rd	4th	5th	Charge	Discharge
	Real	90	90	90	90	90	30	30	30	30	30		
Initial SOC 40%	CC	100	100	100	100	100	40	40	40	40	40	10%	10%
	EKF	97	89	88.5	88.5	92.5	31	28	29	29.5	29.5	2.7%	1%
	UKF	97	91	90.4	90	90	32.5	31	30	30	30	1.68%	0.7%
Initial SOC 50%	CC	110	110	110	110	110	50	50	50	50	50	20%	20%
	EKF	107	88	89	88	88	31	29	29	30	29	4.8%	0.8%
	UKF	105	95	91	91	90	36	32	31	30	30	2.4%	1.8%

This analysis of the SOC level parameter of the BMS, through this comparison of the used estimation methods which is shown in Tables 1 and 2, meets the aim and objective of conducting a comprehensive review of the traditional and modern estimation methods. This concludes that, when comparing the traditional estimation methods with the modern methods, it is evident that the advanced versions of the KF methods are preferred as they are more accurate and adaptive in estimating the SOC and SOH in real-time with frequent variances in the system to work with. While the proposed BMS demonstrates effective real-time tracking, future enhancements could explore lightweight or hybrid filtering techniques to further minimise latency. Such improvements would enhance the system's applicability in scenarios with exceptionally high demands on response time, such as high-congestion environments.

It is recommended that, based on the research conducted and the promising results shown in this project report, the modern estimation method is preferable as an advanced BMS for use in an EV if the user requires extremely accurate tracking and estimation of the battery parameters. As the KF-based EKF method is more accurate than the CC method, but not compared to UKF, as the EKF handles the non-linear system by linearising it but tends to lead to more errors appearing in the system when faced with high levels of non-linearities in the system. Whereas the UKF is more robust at handling high non-linearities, hence being more accurate and efficient at handling complex behaviours in the system. The UKF method also shows consistency in estimation and stability compared to the EKF when faced with high non-linearity. It also presents better accuracy when it comes to dealing with high dimensional systems which consist of dealing with large number of data points. Currently, based on the research conducted and the achieved results, the UKF is the most optimum method for SOC and SOH estimation as it is more robust and adaptable than the other proposed methods. However, the modern estimation method can also be complex to implement as it is a mathematical model-based method. The KF-based methods EKF and UKF use complex computations such as Jacobian matrix and unscented transformation sigma points which demand high computation power, and these increase the cost of the manufacturing and operating costs of the BMS. If the user wants a cost-efficient option, then a good alternative can be the traditional estimation approach of the CC method which is commonly used because it is simple to implement and use, requiring the least computational power compared to the modern estimation approaches; this excessively reduces the expenses of the physical implementation of it. However, they are not ideal for EV battery state calculation applications as they cannot estimate the SOC and SOH with accuracy and their estimation accuracy further extensively decreases as the battery age increases. Compared to other modern filtering methods, it is prone to error accumulation in it when high variations are introduced in the system and its accuracy is highly dependent on the accuracy of the given previous SOC value. All these characteristics of the traditional estimation method make it not an ideal option if the user is looking for a highly advanced BMS.

While the proposed BMS demonstrates significant advancements in accuracy, adaptability, and integration with the IoT, it is important to recognise certain practical implications and limitations. For instance, the increased computational demands of advanced algorithms may affect system efficiency, and the integration of the IoT and advanced sensors may elevate costs. Additionally, while simulation results validate the system's performance, real-world testing under diverse operational conditions, such as extreme temperatures and high vibrations, remains necessary. These considerations highlight opportunities for future research to further refine and validate the system's capabilities.

5. Future Recommendation

For this project, a single battery cell was used but, in practical application, a larger battery pack is required; hence, the next, future step would be to expand the number of battery cells in the battery pack. However, there are challenges to using a larger battery pack, including the irregularities and inconsistency of constant performance between the large number of cells; some cells may perform better, while others might lag behind. Due to this, there are uneven charge accumulations throughout the cells in the battery pack. Hence, to tackle this problem, a battery cell balancing system (BBS) is essential for a multi-cell Li-ion battery pack used in EV applications, as it plays a critical role in ensuring the uniformity, safety, and longevity of the battery pack while in operation, and it works in conjunction with the BMS to further optimise the battery performance and health, thereby enhancing its reliability and efficiency in energy storage. A BBS tracks the multi-battery cells, which are charging or discharging at different rates, having different SOC levels and redistributing the charge evenly among all the cells to have a similar charge so that the battery can provide a constant smooth performance; hence, before the BBS, the cells charge and the SOC levels are uneven, but after the BBS they are even. The reason charge redistribution is important is to prevent the dominant SOC level cells from overcharging or discharging and accumulating excessive heat which badly affects the battery performance and lifespan. It also increases the risk of battery explosion or damage.

The BBS consists of sensing battery cells using algorithms or controllers for routing charging or discharging current to the cell which is typically conducted by using ASICs (battery sense chips and a system charge controller). The types of battery balancing methods are passive and active battery balancing. In passive battery balancing (PBB), the charge distribution consists of discharging current from one battery cell which has most dominant SOC level to all the other battery cells, producing a naturally balanced charge across all cells in the battery, which will distribute charge even to cells which do not require it. Hence, there is energy wastage. Whereas, in active battery balancing (ABB), it uses an intentionally routed path from the most dominant SOC level cell to the lowest SOC level cell and, due to this selective cell path method and controlled balancing, the battery's charge is more efficiently distributed. Thus, ABB is preferable for large battery applications [26].

6. Conclusions

In conclusion, the significance of a robust and adaptive BMS for EV battery management application that can measure and estimate battery critical parameters for the optimised management of an enhanced battery for performance, safety, and lifespan is emphasised. The critical parameters of a battery, such as the SOC and SOH levels, are estimated by using various estimation techniques, including the traditional technique, the CC method, which tracks and integrates the current of battery to estimate the SOC level, and modern techniques, the KF-based methods which are data-driven approach algorithms which predict the state of system to estimate the SOC and SOH levels. The novelty of the developed BMS is characterised in this paper as robust, adaptable, optimised for performance and enhanced longevity, sustainable, cost-efficient, and conducts a comprehensive evaluation of the various estimation techniques. The BMS continuously updates the new estimated state of the battery while extensively adapting to improve the accuracy of the BMS. Additionally, it also minimises the degradation of the battery's internal components throughout its operational lifespan to enhance its performance and its lifespan, thereby reducing battery wastage and reducing costs related to battery maintenance and replacement. The results the comprehensive and analytical evaluation of the developed BMS with the Simulink simulation and ThingSpeak IoT platforms demonstrated that, compared to traditional estimation techniques, the modern technique, the UKF method, achieves a higher level of accuracy at estimating the battery SOC and SOH levels. For battery SOC level estimation, the average estimated SOC for a fully charged battery is 90% and for a fully discharged battery is 30%. The error margin for the UKF method-based BMS in tracking the real battery SOC level, compared to the estimated SOC level, is 1% for a battery charging state and 0.32% for a battery discharging state. Overall, the UKF method is the proposed estimation technique for an advanced and robust BMS for application in real-world scenarios for optimum and efficient EV battery management application. Future studies will focus on evaluating the proposed BMS across different EV categories, including passenger vehicles, commercial fleets, and heavy-duty applications. Such an exploration will ensure that the system meets the diverse operational and performance needs of various EV types.

Author Contributions: M.T.M.N.: conceptualisation, methodology, software, validation, formal analysis, investigation, data curation, writing—original draft, visualisation. M.H.F.: writing—review and editing, visualisation, supervision. N.S.: project administration, writing—review and editing, visualisation, supervision. All authors have read and agreed to the published version of the manuscript.

Funding: This research received no external funding.

Data Availability Statement: No data was used for the research discussed in this article.

Acknowledgments: The author would like to sincerely thank the project supervisor Nagham Saeed and Mohammad Hossein Fouladfar for their guidance and supervision during the period of the project. The authors would also acknowledge the scholars whose articles and books were used as a reference for the research of the project's solutions. The authors are also grateful to Kevin Munisami for providing basic knowledge on how to compose the project report. The authors are also thankful for the help and support of colleagues during the project research.

Conflicts of Interest: The authors declare no conflicts of interest.

Abbreviations

A	Amps
AC	Alternative current
BMS	Battery management system
BBS	Battery balancing system
C	Celsius
CC	Coulomb counting
CO_2	Carbon dioxide
DC	Direct current
ECM	Equivalent circuit modelling
EV	Electric vehicle
EKF	Extended Kalman filter
I	Current
IoT	Internet of things
K	Kelvin
KF	Kalman filter
Li-ion	Lithium-ion
LoRa	Long range
MQTT	Message queue telemetry transport

Ah	Ampere-hour
OCV	Open circuit voltage
R_{EOL}	End-of-life resistance
R_{fresh}	Initial internal resistance
S	Second
SOC	State of charge
SOH	State of health
UKF	Unscented Kalman filter
V	Voltage
WAN	Wide area network

References

1. Battery 2030: Resilient, Sustainable, and Circular. Available online: https://www.mckinsey.com/industries/automotive-and-assembly/our-insights/battery-2030-resilient-sustainable-and-circular (accessed on 1 April 2024).
2. Can Lithium Batteries Be Recycled. Available online: https://www.continentalbattery.com/blog/can-lithium-batteries-be-recycled#:~:text=Yes,%20lithium%20and%20lithium-ion,in%20the%20world%20are%20recycled (accessed on 1 April 2024).
3. The Crucial Role of Managing End-of-Life Li-Ion Battery Sustainability. Available online: https://www.idtechex.com/en/research-article/the-crucial-role-of-managing-end-of-life-li-ion-battery-sustainability/30302 (accessed on 1 April 2024).
4. Crowter, R.; Saeed, N. Designing and Implementation of Simple Wireless Battery Monitoring System for Photovoltaic Application. In Proceedings of the 2023 WF-IoT Conference, Aveiro, Portugal, 12–27 October 2023. Available online: https://www.proceedings.com/content/074/074802webtoc.pdf (accessed on 1 April 2024).
5. Sasirekha, P.; Sneka, E.; Velmurugan, B.; Hameed, M.S.; Sivasankar, P. A Battery Monitoring System based on IoT for Electric Vehicles. In Proceedings of the 2023 5th International Conference on Smart Systems and Inventive Technology (ICSSIT), Tirunelveli, India, 23–25 January 2023; pp. 204–210. [CrossRef]
6. BU-808: How to Prolong Lithium-Based Batteries. Available online: https://batteryuniversity.com/article/bu-808-how-to-prolong-lithium-based-batteries (accessed on 1 April 2024).
7. Wang, S.; Liu, K.; Wang, Y.; Stroe, D.; Fernandez, C.; Guerrero, J. *Multidimensional Lithium-Ion Battery Status Monitoring*, 1st ed.; CRC Press: Milton Park, UK, 2022; pp. 102–150.
8. Xiong, R.; Shen, W. *Advanced Battery Management Technologies for Electric Vehicles*, 1st ed.; Wiley: Hoboken, NJ, USA, 2018; pp. 95–130.
9. Modelling Li-Ion Batteries with Equivalent Circuit Technology. Available online: https://www.powerelectronicsnews.com/modeling-li-ion-batteries-with-equivalent-circuit-technology/#:~:text=Equivalent%20circuit%20modeling%20provides%20a,characteristics%20of%20the%20battery's%20behavior (accessed on 1 April 2024).
10. Equivalent Circuit Models and State-Space Models. Available online: https://www.monolithicpower.com/en/learning/mpscholar/battery-management-systems/battery-modeling/equivalent-circuit-models-and-state-space-models (accessed on 1 April 2024).
11. The State of Charge Estimating Methods for Battery: A Review. Available online: https://onlinelibrary.wiley.com/doi/10.1155/2013/953792 (accessed on 1 April 2024).
12. SOC Estimation by Coulomb Counting. Available online: https://www.batterydesign.net/soc-estimation-by-coulomb-counting/ (accessed on 1 April 2024).
13. A Closer Look at State of Charge (SOC) and State of Health (SOH) Estimation Techniques for Batteries. Available online: https://www.analog.com/en/resources/technical-articles/a-closer-look-at-state-of-charge-and-state-health-estimation-tech.html (accessed on 1 April 2024).
14. BU-902: How to Measure Internal Resistance. Available online: https://batteryuniversity.com/article/bu-902-how-to-measure-internal-resistance#:~:text=NIMH%20packs%20of%206%2018650,when%20they%20reach%20800%20milliohms (accessed on 1 April 2024).
15. How to Measure the Internal Resistance of a Battery. Available online: https://www.instructables.com/How-to-measure-the-internal-resistance-of-a-batter/ (accessed on 1 April 2024).
16. Azis, N.A.; Joelianto, E.; Widyotriatmo, A. State of Charge (SoC) and State of Health (SoH) Estimation of Lithium-Ion Battery Using Dual Extended Kalman Filter Based on Polynomial Battery Model. In Proceedings of the 2019 6th International Conference on Instrumentation, Control, and Automation (ICA), Bandung, Indonesia, 31 July–2 August 2019; pp. 88–93. [CrossRef]
17. Introduction to Kalman Filter and Its Applications. Available online: https://www.intechopen.com/chapters/63164 (accessed on 1 April 2024).
18. Kalman Filter Explained Simply. Available online: https://thekalmanfilter.com/kalman-filter-explained-simply/#:~:text=The%20Kalman%20Filter%20uses%20the,is%20populated%20with%20differential%20equations (accessed on 1 April 2024).
19. SOC Estimator (Kalman Filter). Available online: https://uk.mathworks.com/help/simscape-battery/ref/socestimatorkalmanfilter.html?searchHighlight=EKF%20Estimator&s_tid=srchtitle_support_results_5_EKF%20Estimator (accessed on 1 April 2024).
20. Battery State-of-Health Estimation. Available online: https://uk.mathworks.com/help/simscape-battery/ug/battery-state-of-health-estimation.html (accessed on 1 April 2024).

21. IoT Based Battery Status Monitoring System Using ESP8266. Available online: https://how2electronics.com/iot-based-battery-status-monitoring-system-using-esp8266/ (accessed on 1 April 2024).
22. Lithium-ion Battery Degradation: How to Model It. Available online: https://pubs.rsc.org/en/content/articlehtml/2022/cp/d2cp00417h (accessed on 1 April 2024).
23. Passerini, S.; Bresser, D.; Moretti, A.; Varzi, A. *Batteries Present and Future Energy Storage Challenges*, 1st ed.; Wiley: Hoboken, NJ, USA, 2020; pp. 99–120.
24. How a Battery Works. Available online: https://www.science.org.au/curious/technology-future/batteries (accessed on 1 April 2024).
25. How Do Temperature, Age, and Discharge Rate Affect Battery Run Time. Available online: https://www.keysight.com/blogs/en/tech/bench/2023/07/11/how-do-key-factors-affect-battery-run-time (accessed on 1 April 2024).
26. What Is Battery Balancing and Does Your System Need It. Available online: https://resources.system-analysis.cadence.com/blog/what-is-battery-balancing-and-does-your-system-need-it (accessed on 1 April 2024).